ARL-TR-8076● JULY 2017

US Army Research Laboratory

Detection of Metallic and Electronic Radar Targets by Acoustic Modulation of Electromagnetic Waves

by Gregory J Mazzaro, Andrew J Sherbondy, Matthew R Judy, Kyle A Gallagher

NOTICES

Disclaimers

The findings in this report are not to be construed as an official Department of the Army position unless so designated by other authorized documents.

Citation of manufacturer's or trade names does not constitute an official endorsement or approval of the use thereof.

Destroy this report when it is no longer needed. Do not return it to the originator.

ARL-TR-8076● JULY 2017

US Army Research Laboratory

Detection of Metallic and Electronic Radar Targets by Acoustic Modulation of Electromagnetic Waves

by Gregory J Mazzaro
The Citadel, The Military College of South Carolina, Charleston, SC

Andrew J Sherbondy and Matthew R Judy
Oak Ridge Associated Universities, Oak Ridge, TN

Kyle A Gallagher
Sensors and Electron Devices Directorate, ARL

REPORT DOCUMENTATION PAGE

Form Approved
OMB No. 0704-0188

1. REPORT DATE *(DD-MM-YYYY)*	2. REPORT TYPE	3. DATES COVERED (From - To)
July 2017	Technical Report	26 June 2017–11 August 2017

4. TITLE AND SUBTITLE
Detection of Metallic and Electronic Radar Targets by Acoustic Modulation of Electromagnetic Waves

5a. CONTRACT NUMBER

5b. GRANT NUMBER

5c. PROGRAM ELEMENT NUMBER

6. AUTHOR(S)
Gregory J Mazzaro, Andrew J Sherbondy, Matthew R Judy, Kyle A Gallagher

5d. PROJECT NUMBER
GTSPO#-17-123Mod1

5e. TASK NUMBER

5f. WORK UNIT NUMBER

7. PERFORMING ORGANIZATION NAME(S) AND ADDRESS(ES)
US Army Research Laboratory
ATTN: RDRL-SER-U
2800 Powder Mill Road, Adelphi, MD 20783-1197

8. PERFORMING ORGANIZATION REPORT NUMBER
ARL-TR-8076

9. SPONSORING/MONITORING AGENCY NAME(S) AND ADDRESS(ES)

10. SPONSOR/MONITOR'S ACRONYM(S)

11. SPONSOR/MONITOR'S REPORT NUMBER(S)

12. DISTRIBUTION/AVAILABILITY STATEMENT
Approved for public release; distribution is unlimited.

13. SUPPLEMENTARY NOTES

14. ABSTRACT
Acoustic-electromagnetic (EM) interaction is evaluated for metallic and electronic target detection. The transmitter consists of a radar-wave generator emitting a single EM frequency and an acoustic-wave generator emitting a single acoustic frequency. The EM wave and the acoustic wave interact at the target. The target reradiates a new EM wave, which consists of the original EM wave modulated by the acoustic wave. This reradiated wave is captured by the radar's receive antenna. The presence of measurable EM energy at any discrete multiple of the audio frequency away from the original radio-frequency (RF) carrier indicates target detection. Proof-of-concept detection is demonstrated for purely metallic and RF electronic targets within the near field of an ultra-wideband radar antenna operating in the ultra-high frequency band.

15. SUBJECT TERMS
radar, acoustic, electromagnetic, wave, interaction, modulation, detection, metallic, electronic, nonlinear, junction

16. SECURITY CLASSIFICATION OF:			17. LIMITATION OF ABSTRACT	18. NUMBER OF PAGES	19a. NAME OF RESPONSIBLE PERSON
a. REPORT	b. ABSTRACT	c. THIS PAGE			19b. TELEPHONE NUMBER (Include area code)
Unclassified	Unclassified	Unclassified	UU	26	Kelly D Sherbondy (301) 394-2533

Contents

List of Figures

1. Introduction

Detection of radio-frequency (RF) electronics—targets whose radar cross sections (RCSs) are too small to be seen by traditional radar—has recently been investigated by implementing nonlinear (or "harmonic") radar.[1] This novel type of radar relies on the presence of electromagnetic (EM) nonlinearities in the target to convert EM energy incident on the target at an original set of frequencies into EM energy reradiated from the target at a new set of frequencies (e.g., harmonics). Reception of frequencies different from the original transmit set indicates target detection.

For nonlinear radar, the physical phenomenon that produces a measureable target response is purely EM. The radar generates an EM wave from its transmit antenna, the target is illuminated by a weaker copy of the transmitted EM wave, the target reradiates another EM wave, and the radar captures a weaker copy of the reradiated EM wave at its receive antenna. The conversion of the EM energy, from the illuminating waveform from an original frequency set into new EM energy reradiated at a new frequency set, occurs at the semiconductor and/or metal-to-metal junctions[2] in the target. These junctions distort the transmitted EM waveform into a new reradiated waveform, which contains Fourier components that were not part of the original transmission.

In this work, a different physical phenomenon is evaluated for target detection: the distortion of an EM wave caused by the interaction of an acoustic (audible, pressure) wave and the original (unmodulated) EM wave. The hybrid acoustic-EM technique is illustrated in Fig. 1. The radar transmitter (Tx) consists of an EM wave generator (i.e., a transmit antenna) emitting a single EM frequency f_{RF} and an acoustic-wave generator (here depicted as a speaker) emitting a single acoustic frequency f_{audio} . At the device under test (DUT), the EM wave and the acoustic wave interact. The target reradiates a new EM wave, which consists of the original EM wave modulated by the acoustic wave. The new EM wave contains a set of frequencies $f_{RF} \pm n \cdot f_{audio}$, where n is any positive integer. This reradiated wave is captured by the radar receiver (Rx). The presence of measurable EM energy at any discrete multiple of f_{audio} away from the original RF carrier f_{RF} (i.e., at any $n \neq 0$) indicates target detection.

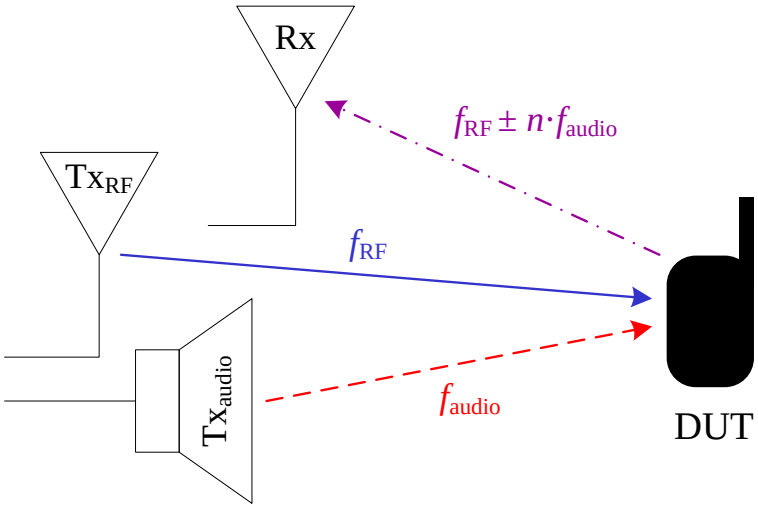

Fig. 1 Hybrid acoustic/EM technique for remotely detecting RF electronic targets: the transmitter consists of an EM-wave generator (antenna) and an acoustic-wave generator (speaker); a second antenna receives the EM wave modulated by the acoustic wave.

In this report, 2 ways in which acoustic and EM waves interact at targets of interest are described. Detection of canonical and purely metallic targets is performed by exploiting one type of acoustic-EM interaction. Detection of RF electronic targets is performed by exploiting a second type of acoustic-EM interaction.

2. Acoustic-Electromagnetic Interaction

There are 2 mechanisms described in the available literature by which acoustic waves interact with EM waves at metallic or electronic targets to generate new spectral content in a radar return. Considering the Tx_{RF} and Rx antennas to be the "original" radar system, the acoustic transmitter Tx_{audio} can impart the modulation $\pm n \cdot f_{audio}$ onto the original transmit/receive waveform by 2 fundamentally different physical phenomena: translational motion, which produces a Doppler shift (and harmonics of that shift) in the target reflection, and intermittent metal contact, which interrupts the reflection like a switching transient.

Whether the acoustic wave from the speaker travels over the air or the wave couples into the target from the material around it, the acoustic energy vibrates ("shakes") the target. For a target that is not necessarily a metal, vibration of its surface deforms the outer shell and compresses the inner material. As a result, the original RCS of the target is perturbed. The inner and outer perturbations may be modeled separately.[3] For metal and electronic targets, very little of the radar wave propagates into (and reflects from) the dielectrics beyond the conductors (or semiconductors); thus, only the perturbation of the outer shell (or circuit board) of the target is relevant. This perturbation is depicted in Fig. 2a.

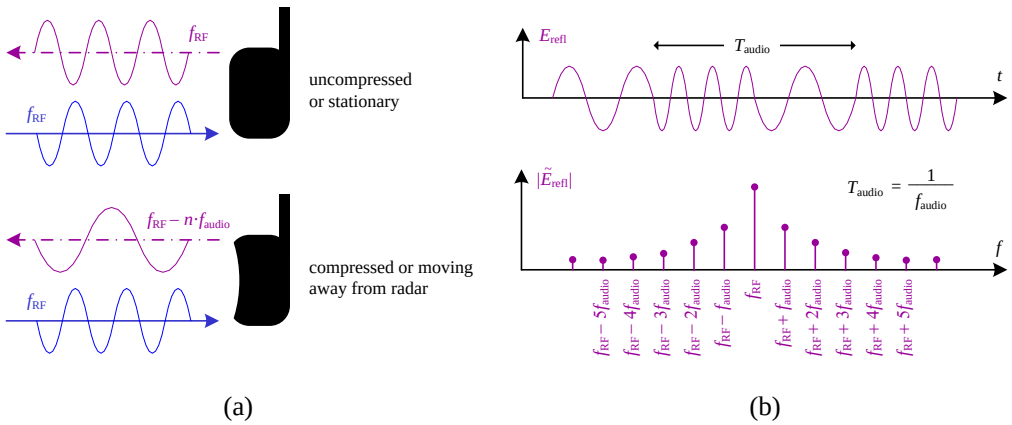

Fig. 2 (a) Frequency modulation imparted onto the EM wave by translational motion (or compression/expansion) of the target and (b) time-domain reflected radar waveform and associated Fourier spectrum

If the radar wave incident on the target is assumed to be a uniform plane wave and the acoustic wave incident on the target produces translational motion in the target, the electric-field intensity reflected by the target E_{refl} may be written as a sinusoid with a phase that is linearly dependent upon the target velocity toward the radar receiver.[4] Thus, the modulation imparted onto the EM wave with carrier frequency f_{RF} is entirely phase modulation.[5]

If the acoustic transmission is a steady tone, the surface of the target vibrates sinusoidally.[6] Since the time derivative of the phase of E_{refl} is generally nonzero, the perturbation imparted by the acoustic source on the target, as a result of moving the target toward and away from the radar receiver sinusoidally, is frequency modulation (FM).

In the Fourier domain, compared to unidirectional translational motion,[7] sinusoidal motion produces a spectral spreading wider than that predicted by Doppler shift alone.[8] This spreading extends both above and below f_{RF}.[9]. Early measurements, using a 10-GHz radar and oscillating 6-inch metal discs, confirmed that the spectral peaks are indeed separated by $\Delta f = f_{audio}$.[10] Since the perturbation of the radar return results in pure FM, the mathematics associated with FM used for radio communications applies, and in the frequency domain, E_{refl} may be written as a series of Fourier components whose amplitudes are Bessel coefficients.[11]

The degree of modulation, and thus the total energy spread across the $n \neq 0$ sidebands, depends on the displacement of the target surface away from its initial ("unshaken") position. Sample FM waveforms are shown in both the time and frequency domains in Fig. 2b.

The greatest Doppler shift occurs when a target moves directly toward or away from the radar. Therefore, with regard to target orientation, the components of E_{refl} are maximum when the target vibrates directly toward or away from the receiver.[12] The reflected response is further enhanced if the incident acoustic energy activates a mechanical resonance, which further displaces the target surface.[13]

Using this Doppler-based mechanical-EM interaction, a hybrid acoustic/radar sensor system was developed for detecting buried landmines.[14] The radar portion of the sensor transmits and receives at 8 GHz.[15] while the acoustic portion of the sensor transmits between 100 Hz and 1 kHz.[16] The acoustic transducer is a mechanical shaker placed in contact with the surface of the material within which the target is buried.[17] To vibrate the target efficiently, the acoustic source needs to be placed within one acoustic wavelength of the material on/in which the target is buried; otherwise, the acoustic waves will propagate only along the surface of the burial material and not reach any appreciable depth.[16]

Experiments have shown that acoustic resonances greatly improve the detectability of shallow-buried landmines.[18] Also, mines possess acoustic resonances, which clutter objects do not.[19] Both metallic and nonmetallic landmines are detectable down to a depth of at least 11 cm.[16] Detection is possible beneath rough surfaces as long as the acoustic spot size illuminating the rough surface is significantly greater than the cross-sectional area of the target.[20]

A secondary effect of shaking the target, which can produce an even stronger return at higher-order sidebands ($n > 1$), is to cause intermittent contact between metal junctions within the target. This phenomenon is depicted in Fig. 3a.

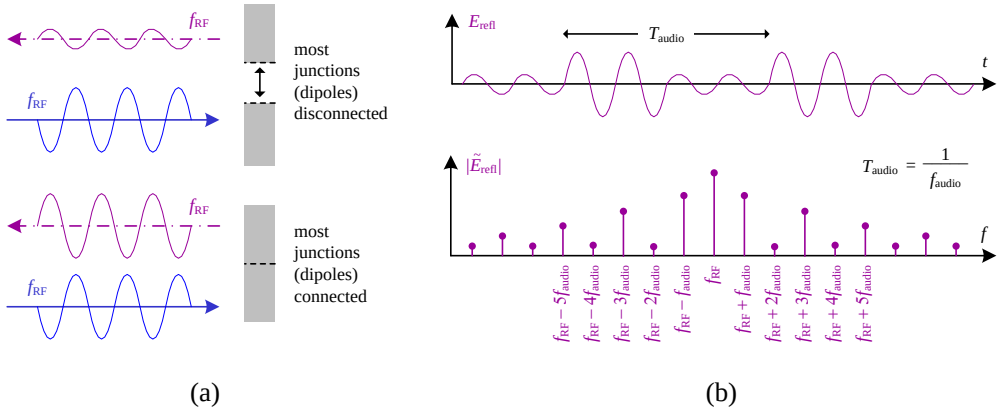

(a) (b)

Fig. 3 (a) Amplitude modulation imparted onto the EM wave by intermittent contact of metal junctions within the target and (b) time-domain reflected radar waveform and associated Fourier spectrum

If a metal or electronic target vibrates while it is being illuminated by an EM wave, the reflected wave will contain not only a Doppler shift due to displacement of the target surface; the target will generate additional spectral content, which resembles noise.[21] Since this spectral content is centered on f_{RF} and also occurs at intervals of $\Delta f = f_{audio}$, it may be considered another form of modulation of the transmitted EM wave by the acoustic wave. This modulation may be described by the interruption of surface currents established along the target.[21] Such interruptions occur at a rate of f_{audio} and may be modeled by time-varying surface impedances.[22]

Alternatively, the acoustic modulation may be modeled by the periodic connection and disconnection of dipole antennas along the target surface; each dipole radiates at f_{RF}.[21] Measurements on $n \neq 0$ sidebands[23] indicate that the dipole-antenna collection may be replaced by a single center-loaded conducting cylinder.[24] Multiple intermittent connections may be replaced by a single time-varying load impedance[25] where the peak radar return occurs when the target (dipole) is short-circuited.[26] Mathematically, the intermittent contact may be described as a square-wave multiplication of the original EM wave.[21] Thus, by vibrating the target to cause intermittent metal-metal contact, the modulation imparted onto the original (stationary-target) EM wave is amplitude modulation (AM).

A sample AM waveform is shown in Fig. 3b along with its corresponding Fourier spectrum. In this case, the degree of modulation depends on the difference between the minimum and maximum load impedance,[26] which physically corresponds to the difference between the number of metal junctions that are connected versus those that are disconnected along/inside the target at any one time.

In the following section, an experiment is described, which confirms that metal and electronic targets of interest may be detected by exploiting either of the 2 aforementioned acoustic-EM interactions.

3. Near-Field Experiment and Data

The experiment used to receive acoustically modulated radar waveforms from metal and electronic targets is shown as a flowchart in Fig 4.

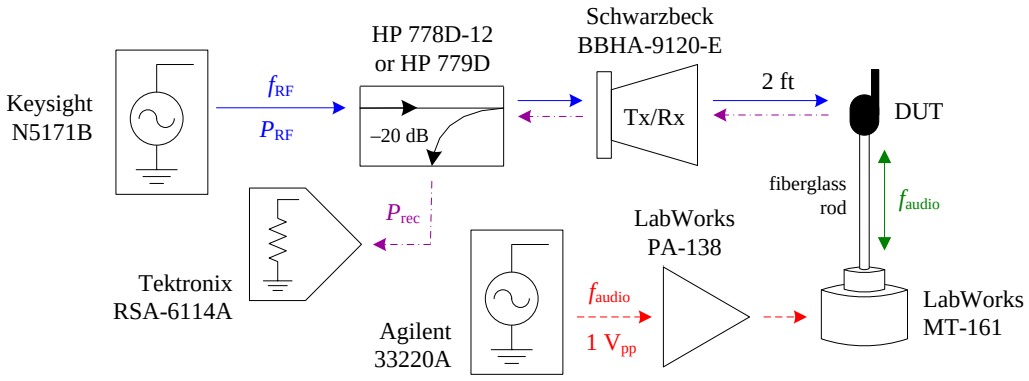

Fig. 4 Flowchart of wireless experiment to receive acoustically modulated radar waveforms.

The RF source is the Keysight N5171B analog signal generator. It outputs a continuous-wave (CW) signal at a frequency f_{RF} and a constant power of P_{RF} = –10 dBm. This CW transmit signal enters a Hewlett Packard (HP) directional coupler and passes on to the transmit antenna. For frequencies less than or equal to 2 GHz, the coupler is the HP 778D-12. For frequencies greater than 2 GHz, the coupler is the HP 779D. The Schwarzbeck BBHA-9120-E horn antenna (oriented for vertical polarization) transmits f_{RF} to the DUT. The distance between the antenna and the target is 2 ft. This short distance is within the near field of the antenna.

The DUT is attached to a 3-ft-long fiberglass rod using a pair of rare-earth magnets at the end of the rod. The other end of the fiberglass rod is attached to the LabWorks MT-161 modal test shaker. The shaker is powered by the LabWorks PA-138 amplifier, into which is fed an audio-frequency signal at f_{audio} provided by the Agilent 33220A function generator. The shaker vibrates the rod, and the rod vibrates the DUT. The EM wave reflected by the DUT (while it is illuminated by f_{RF} and shaking at a frequency of f_{audio}) is received by the same BBHA-9120-E antenna. The backward-traveling reflection is sampled (at –20 dB) by the directional coupler. The sampled P_{rec} is sent from the coupled port to the Tektronix RSA-6114A spectrum analyzer.

Figures 5–7 contain spectra recorded for 3 different targets. The thick (red) traces are the target-present traces. The thin (black) traces are the target-absent traces. The upper pair of spectra correspond to f_{RF} = 800 MHz, the lower pair correspond to f_{RF} = 1000 MHz, the left pair correspond to f_{audio} = 50 Hz, and the right pair correspond to f_{audio} = 100 Hz .

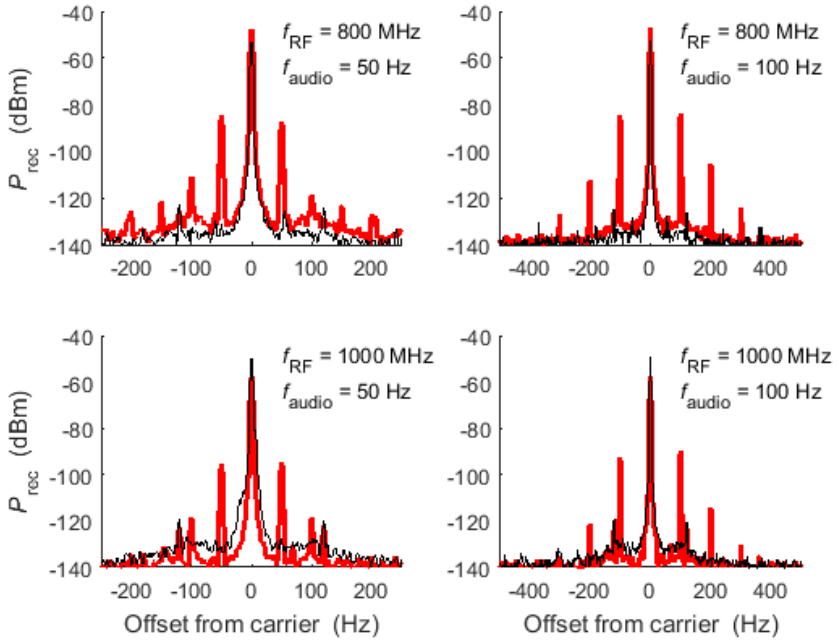

Fig. 5 Spectra recorded using the experiment of Fig. 4: the target is a metallic corner reflector, which measures 18 inches on each side. The thick (red) traces indicate that the target is present. The thin (black) traces indicate that the target is absent.

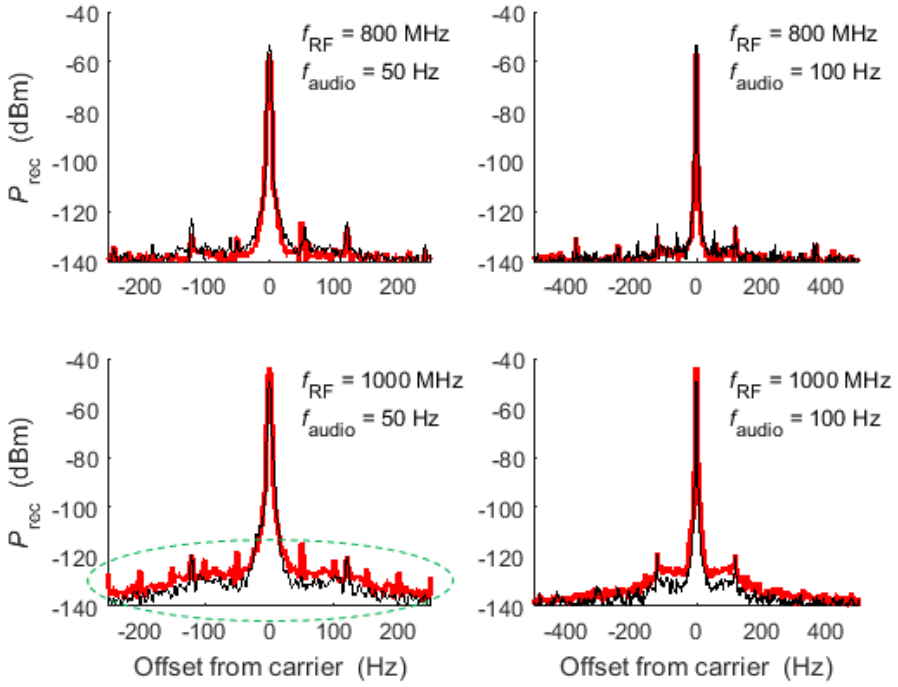

Fig. 6 Spectra recorded using the experiment of Fig. 4: the target is a hollow metallic circular cylinder with a diameter of 6 inches and a height of 8 inches. The top of the cylinder faces the antenna. The top of the cylinder is held loosely to the body of the cylinder (i.e., there is a thin air gap between the top and the body around the perimeter of the top).

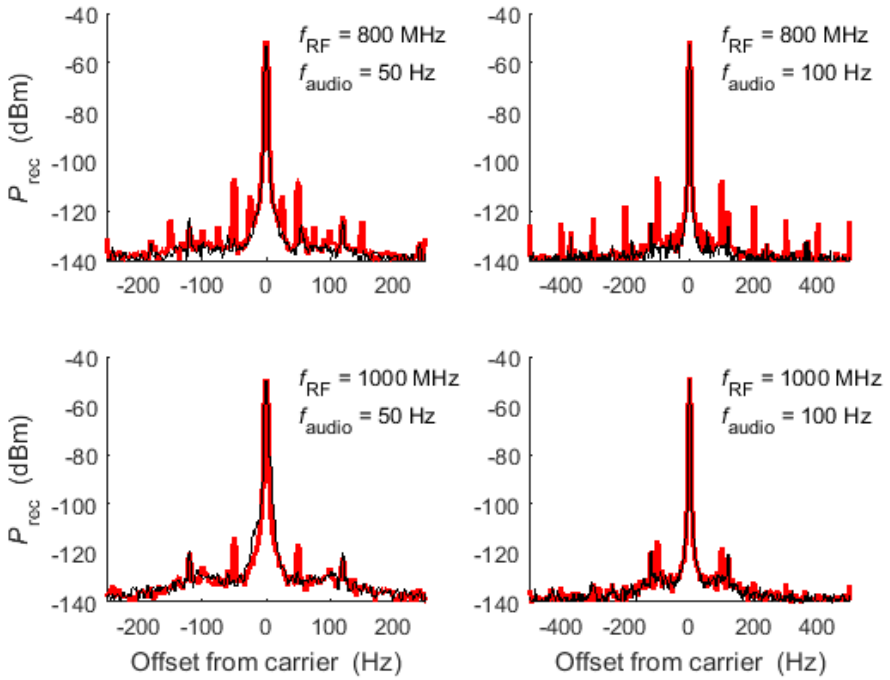

Fig. 7 Spectra recorded using the experiment of Fig. 4: the target is a Motorola MD200R radio, upright and turned sideways to the antenna. The thick (red) traces indicate that the target is present. The thin (black) traces indicate that the target is absent.

The RSA-6114A analyzer is configured to capture spectra centered at f_{RF} with a bandwidth of $10f_{audio}$ (i.e., such that sidebands out to $n = \pm 5$ are visible). The number of frequency points captured across each spectrum trace is 4001. The resolution bandwidth (per frequency point) is 3 Hz. The N5171B, 33220A, and RSA-6114A are controlled using a laptop, programmed in MATLAB using its Instrument Control toolbox and scripts written in Standard Commands for Programmable Instruments (SCPI) code. Communication between the laptop and the instruments is accomplished over a GPIB-USB interface. Code for an example program is provided in the Appendix.

Figure 5 contains 4 spectra recorded for a large metallic corner reflector. At all 4 frequency combinations, the corner reflector is clearly (visibly) detectable above the noise because each target-present case contains $\pm n \cdot f_{audio}$ spikes, which do not appear in each target-absent trace. Figure 6 contains data recorded for a metallic cylinder. Only at f_{RF} = 1,000 MHz and f_{audio} = 50 Hz is there significant spectral energy that appears in the target-present trace that does not appear in the target-absent case. Figure 7 contains data recorded for a handheld radio. At 3 out of the 4 frequency combinations, the radio is detectable. At f_{RF} = 1,000 MHz and f_{audio} = 100 Hz , there is no significant difference between the target-present and target-absent traces.

4. Conclusions

The interaction between acoustic and EM waves appears to be exploitable for detecting metallic and electronic radar targets. Data taken on 3 targets (a corner reflector, a metallic cylinder, and a handheld radio) indicate that EM waves are indeed modulated by acoustic waves at these targets of interest, for particular combinations of radar and acoustic frequencies (at ultra-high frequency and in the audible range, respectively). In a follow-up investigation, we will attempt to achieve target detection at a range of 10 ft, for a wider selection of targets illuminated by a wider range of frequencies.

5. References

1. Mazzaro GJ, Martone AF, K. Ranney I, Narayanan RM. Nonlinear radar for finding RF electronics: System design and recent advancements. IEEE Trans Microw Theory Tech. 2017 May;65(5):1716–1726.
2. Origlio GF. The METRRA techniques. Ft Belvoir (VA): US Army Mobility Equipment Research and Development Center; 1972. AD522716.
3. Lawrence DE, Sarabandi K. Acoustic and electromagnetic wave interaction: Analytical formulation for acousto-electromagnetic scattering behavior of a dielectric cylinder. IEEE Trans Ant Propag. 2001 Oct;49(10):1382–1392.
4. Borkar SR, Yang RF H. Reflection of electromagnetic waves from oscillating surfaces. IEEE Trans Ant Propag. 1975 Jan;23(1):122–127.
5. Kleinman RE, Mack RB. Scattering by linearly vibrating objects. IEEE Trans Ant Propag. 1979 May;27(3):344–352.
6. Wetherington JM, Steer MB. Standoff acoustic modulation of radio frequency signals in a log-periodic dipole array antenna. IEEE Ant Wireless Propag Lett. 2012;(11):885–888.
7. De Zutter D. Doppler effect from a transmitter in translational motion. IEEE J Microwaves, Opt Acoust. 1979 Mar;3(2): 85–92.
8. Kleinman RE. Electromagnetic scattering by a linearly oscillating target. Hascom AFB (MA): Air Force Cambridge Research Laboratory; 1975 Oct. Report No.: AFCRL-TR-75-0554.
9. Cooper J. Scattering of electromagnetic fields by a moving boundary: The one-dimensional case. IEEE Trans Ant Propag. 1980 Nov;28(6):791–795.
10. Mack RB. Measured backscatter modulation from linearly oscillating metal disks. Griffiss AFB (NY): Rome Air Development Center; 1977 Aug. Report No.: RADC-TR-77-285.
11. Van Bladel J. De Zutter D. Reflections from linearly vibrating objects: Plane mirror at normal incidence. IEEE Trans Ant Propag. 1981 July;29(4):629–637.
12. De Zutter D. Reflections from linearly vibrating objects: Plane mirror at oblique incidence. IEEE Trans Ant Propag. 1982 Sept;30(5):898–903.

13. Sarabandi K, Lawrence DE. Acoustic and electromagnetic wave interaction: Estimation of doppler spectrum from an acoustically vibrated metallic circular cylinder. IEEE Trans Ant Propag. 2003 July;51(7):1499–1507.

14. Scott WR, Schroeder C, Martin JS. An acousto-electromagnetic sensor for locating land mines. In: Proc SPIE 3392; 1998 Apr. p. 176–186.

15. Scott WR, Schroeder C, and Martin JS. A hybrid acoustic/electromagnetic technique for locating land mines. In Proc Int Geosci Remote Sens. Symp; 1998 July. p. 216–218.

16. Scott WR, Larson GD, Martin JS. Simultaneous use of elastic and electromagnetic waves for the detection of buried land mines. In Proc SPIE 4038; 2000 Apr. p. 667–678.

17. Scott WR, Martin JS. An experimental model of a acousto-electromagnetic sensor for detecting land mines. In Proc. IEEE Ant Propag Soc Int Symp; 1998 June. p. 978–981.

18. Scott WR, Martin JS. Experimental investigation of the acousto-electromagnetic sensor for locating land mines. In Proc SPIE 3710; 1999 Apr. p. 204–214.

19. Scott WR, Martin JS, Larson GD. Investigation of a technique that uses elastic waves to detect buried land mines. In Proc Int Geosci Remote Sens Symp; 2000 July. p. 1640–1642.

20. Lawrence DE, Sarabandi K. Acousto-electromagnetic interaction in the detection of buried objects. In Proc Int Geosci Remote Sens Symp; 2001 July. p. 1989–1991.

21. Bahr AJ, Frank VR, Petro JP, Sweeney LE. Radar scattering from intermittently contacting metal targets. IEEE Trans. Ant Propag. 1977 July;25(4):512–518.

22. Lawrence DE, Sarabandi K. "Electromagnetic scattering from vibrating metallic objects using time-varying generalized impedance boundary conditions. In Proc IEEE Ant Propag Soc Int Symp; 2002 June. p. 782–785.

23. Bahr AJ, Petro JP. Frequency dependence of the modulated scattering from simple intermittently contacting metal targets. In Proc Ant Propag Soc Int Symp; 1977 June. p. 166–168.

24. Hu Y. Back-scattering cross section of a center-loaded cylindrical antenna. IRE Trans Ant Propag. 1958 Jan;6(1):140–148.

25. FrankVR. Petro JP, BahrAJ. Backscattering from a cylindrical dipole centrally loaded by a time-varying impedance. IEEE Trans Ant Propag. 1977 May;25(3):356–358.

26. Bahr AJ. Petro JP. On the RF frequency dependence of the scattered spectral energy produced by intermittent contacts among elements of a target. IEEE Trans Ant Propag. 1978 July;26(4):618–621.

Appendix. Code for an Example Program

Provided in this Appendix is a MATLAB script, which uses the Instrument Control toolbox to configure the signal generation and capture equipment in Fig. 4. The output from the script is a power-versus-frequency plot in the style of Figs. 5–7.

```
freq_RF = 800e6;     % radio frequency
pwr_RF_dBm = -10;

freq_audio = 100;    % audio frequency
Vpp_audio = 1.0;

res_bw = 3;                     % spectrum analyzer
freq_span = freq_audio * 10;    % settings
freq_pts = 4001;
hold_count = 10;
yscale_ref = -15;
yscale_offset = -40;
yscale_dB = 100;

%%%%%%%%%%%%%%%%%%%%%%%%%%%%%%%%%%%%%%%%%%%%%%%%%%%%%%%%%%%%%%%%
%%% configure Keysight N5171B signal generator %%%
%%%%%%%%%%%%%%%%%%%%%%%%%%%%%%%%%%%%%%%%%%%%%%%%%%%%%%%%%%%%%%%%

exg = gpib('ni', 0, 19);

fopen(exg);
fwrite(exg,['OUTPut:MODulation:STATe OFF']);
fwrite(exg,['POWER ' num2str(pwr_RF_dBm) 'dBm']);
fwrite(exg,['FREQ ' num2str(freq_RF) 'Hz']);
fwrite(exg,['OUTPut:STATe ON']);
fclose(exg);

pause(0.5)
```

```
%%%%%%%%%%%%%%%%%%%%%%%%%%%%%%%%%%%%%%%%%%%%%%%%%%%%%%%%%%%%
%%% configure Agilent 33220A function generator %%%
%%%%%%%%%%%%%%%%%%%%%%%%%%%%%%%%%%%%%%%%%%%%%%%%%%%%%%%%%%%%

awg = gpib('ni', 0, 10);
set(awg,'OutputBufferSize',2^18);
set(awg,'Timeout',40.0);

fopen(awg);
fprintf(awg, ['FUNCtion SINusoid']);
fprintf(awg, ['FREQuency ' num2str(freq_audio)]);
fprintf(awg, ['VOLTage ' num2str(Vpp_audio)]);
fprintf(awg, ['OUTPut ON']);
fclose(awg);

pause(0.5);

%%%%%%%%%%%%%%%%%%%%%%%%%%%%%%%%%%%%%%%%%%%%%%%%%%%%%%%%%%%%
%%% configure Tektronix RSA-6114A spectrum analyzer %%%
%%%%%%%%%%%%%%%%%%%%%%%%%%%%%%%%%%%%%%%%%%%%%%%%%%%%%%%%%%%%

sa = gpib('ni', 0, 1);
set(sa,'InputBufferSize',2^20);
set(sa,'Timeout',20);

fopen(sa);

fprintf(sa,['SENSE:SPECTRUM:BANDWIDTH:RESOLUTION ' num2str(res_bw)
'Hz']);
fprintf(sa,['SENSE:SPECTRUM:FREQUENCY:CENTER  '  num2str(freq_RF)
'Hz']);
fprintf(sa,['SENSE:SPECTRUM:FREQUENCY:SPAN  '  num2str(freq_span)
'Hz']);
fprintf(sa,['SENSE:SPECTRUM:POINTS:COUNT P' num2str(freq_pts)]);
fprintf(sa,['INPUT:RLEVEL ' num2str(yscale_ref)]);
```

```
fprintf(sa,['DISPLAY:SPECTRUM:Y:SCALE:OFFSET                    '
num2str(yscale_offset)]);
fprintf(sa,['DISPLAY:SPECTRUM:Y:SCALE ' num2str(yscale_dB)]);


fprintf(sa,['INITIATE:CONTINUOUS OFF']);


fprintf(sa,['TRACE1:SPECTRUM:FUNCTION AVERage']);
fprintf(sa,['TRACE1:SPECtrum:AVERage:COUNt                      '
num2str(hold_count)]);
fprintf(sa,['TRACE1:SPECtrum:AVERage:RESet']);


fprintf(sa,['INITIATE:IMMEDIATE']);
fprintf(sa,'READ:SPECtrum:TRACe1?');


char(fread(sa,1));
ndig = str2double(char(fread(sa,1)));
nbytes = str2double(char(fread(sa,ndig))');
P_rec = (fread(sa,nbytes/4,'single'))';


fprintf(sa,['INITIATE:CONTINUOUS ON']);
fprintf(sa,['TRACE1:SPECTRUM:FUNCTION NONE']);
fprintf(sa,['INITIATE:IMMEDIATE']);


fclose(sa);


pause(0.5);


%%%%%%%%%%%%%%%%%%%%%%%%%%%%%%%%%%%%%%%%%%%%%%%%
%%% turn N5171B and 33220A outputs off %%%
%%%%%%%%%%%%%%%%%%%%%%%%%%%%%%%%%%%%%%%%%%%%%%%%


fopen(awg);
fprintf(awg, ['OUTPut OFF']);
fclose(awg);
```

```
fopen(exg);
fwrite(exg,['OUTPut:STATe OFF']);
fclose(exg);

%%%%%%%%%%%%%%%%%%%%%%%%%%%%%%%%%%%%%%%%%%%%%%%%
%%% plot spectrum recorded by RSA-6114A %%%
%%%%%%%%%%%%%%%%%%%%%%%%%%%%%%%%%%%%%%%%%%%%%%%%

delta_f = freq_span / (freq_pts-1);
f_start = freq_RF - freq_span/2;
f_end = freq_RF + freq_span/2;
freq = f_start:delta_f:f_end;

figure
plot(freq-freq_RF,P_rec)
axis([-Inf -140 0])
ylabel('Received Power,  {\itP}_{rec}  (dBm)')
xlabel('Frequency Offset from Carrier  (Hz)')
grid
```

List of Symbols, Abbreviations, and Acronyms

AM	amplitude modulation
CW	continuous-wave
DUT	device under test
EM	electromagnetic
FM	frequency modulation
HP	Hewlett Packard
RCS	radar cross section
RF	radio frequency
Rx	radar receiver
SCPI	Standard Commands for Programmable Instruments
Tx	radar transmitter
USB	universal serial bus

1 (PDF) DEFENSE TECHNICAL INFORMATION CTR DTIC OCA

2 (PDF) DIRECTOR US ARMY RESEARCH LAB RDRL CIO L IMAL HRA MAIL & RECORDS MGMT

1 (PDF) GOVT PRINTG OFC A MALHOTRA

8 (PDF) DIRECTOR US ARMY RESEARCH LAB RDRL SER U
K GALLAGHER
M JUDY
A MARTONE
G MAZZARO
K RANNEY
A SHERBONDY
K SHERBONDY
A SULLIVAN

INTENTIONALLY LEFT BLANK.